ANALYSIS OF THE PROCESSING OF NASHVILLE URBAN EMISSIONS ON JULY 3 AND JULY 18, 1995

P. H. Daum, L. Kleinman, D. G. Imre, L. J. Nunnermacker,
Y.-N. Lee, S. R. Springston, and L. Newman
Environmental Chemistry Division
Department of Applied Science
Brookhaven National Laboratory
Upton, NY 11973

J. Weinstein-Lloyd
Dept. of Chemistry and Physics
SUNY, Old Westbury
Old Westbury, NY 11586

Analysis of the processing of Nashville urban emissions on July 3 and July 18, 1995

P. H. Daum, L. Kleinman, D. G. Imre, L. J. Nunnermacker, Y.-N. Lee,
S. R. Springston, and L. Newman

Environmental Chemistry Division, Department of Applied Science, Brookhaven National Laboratory, Upton, New York

J. Weinstein-Lloyd

Dept. of Chemistry and Physics, State University of New York, Old Westbury, New York

Abstract. This paper analyzes data obtained on July 3 and 18, 1995, during the summer 1995 Southern Oxidant Study (SOS) field campaign. In a previous paper [*Nunnermacker et al.*, 1998] we analyzed measurements of key species that contribute to formation of O_3 in the Nashville urban plume and presented a semiquantitative picture of O_3 production in the plume from the point of emission to locations where no net O_3 was being formed. In this paper we use a box model constrained by observed concentrations of stable species to obtain a detailed mechanistic description of the instantaneous processing of urban emissions at various times in the chemical evolution of the urban plume. Instantaneous ozone production rates and efficiencies with respect to NO_x and to primary radical production are examined. At high NO_x concentrations in the fresh urban plume the O_3 production rate was found to be directly proportional to the hydrocarbon to NO_x reactivity ratio. At lower NO_x concentrations, corresponding to the mature urban plume and the background atmosphere, the O_3 production rate was found to be directly proportional to the NO_x concentration and independent of the hydrocarbon reactivity. NO_x was found to be most efficiently used for ozone production at low NO_x concentrations. In contrast, the efficiency with which the system uses primary radicals was found to be very low at low NO_x concentrations and to peak at a NO_x concentration of approximately 4 ppbv. A sensitivity study of the instantaneous O_3 production rates to changes in NO_x or hydrocarbon concentrations showed that the instantaneous O_3 production rate at the center of the urban plume, when half of the urban NO_x emissions had been processed, is hydrocarbon sensitive. However, O_3 production becomes NO_x sensitive as the plume matures.

1. Introduction

This paper analyzes data obtained July 3 and 18 during the 1995 Southern Oxidant Studies (SOS) field campaign when the meteorological flows were particularly well defined and from a direction that made possible a study of the Nashville urban plume in the absence of the direct influence of emissions from the many power plants in the area. In a previous publication [*Nunnermacker et al.*, 1998] we presented the data for these two days and performed an analysis aimed at deriving a semiquantitative picture of O_3 formation in the urban plume, from close to the source region to locations where virtually no net O_3 was being produced. The focus of this analysis was to obtain estimates of O_3 production rates, to determine the efficiency with which Nashville NO_x emissions were utilized to form O_3, and to examine the importance of anthropogenic and biogenic hydrocarbons for O_3 production in the urban plume. We found that photochemical processing in the Nashville urban plume was very rapid. On the basis of our analysis we inferred an average OH concentration of 1.2×10^7 molecules cm^{-3} which caused half the emitted NO_x and slightly more than half the emitted anthropogenic hydrocarbons to be consumed within the first 2 hours after emission. The average O_3 production rate from time of emission to the point at which the plume was sampled was found to be ~10 ppbv/h. Each emitted NO_x molecule was found to produce between 2.5 and 4 molecules of O_3. Anthropogenic hydrocarbons were found to be the most

important source of hydrocarbons during the early stages of O_3 formation in the urban plume. Biogenic hydrocarbons increased in importance as the plume aged and mixed with background air, so by the time O_3 production was complete, contributions of biogenic and anthropogenic hydrocarbons to O_3 production were nearly equal.

Here we use a photochemical box model constrained by measured trace gas concentrations to produce a detailed mechanistic description of the instantaneous processing of the urban emissions at the various locations where the plume was sampled. Quantities calculated include instantaneous-radical concentrations, O_3 production rates, and O_3 production efficiencies with respect to NO_x and with respect to radicals. The model is also used to investigate the sensitivity of the instantaneous O_3 production rate to changes in NO_x or hydrocarbon concentrations.

As part of this analysis of instantaneous chemistry in the Nashville urban plume, we have derived analytic formulas for the O_3 production efficiency with respect to NO_x and with respect to radicals. These efficiencies are the number of O_3 molecules produced per NO_x molecule oxidized and per free radical created from photolysis reactions. Also, we derive a formula for the rate of O_3 production that reduces to the high NO_x limit given by *Sillman et al.* [1990]. These formulas follow in a straightforward way from the photochemical rate equations and from previously published expressions for O_3 production rates [i.e., *Sillman et al.*, 1990, 1995; *Kleinman et al.*, 1998], but to the best of our

knowledge have not been previously reported. It should be emphasized that the formulations and analysis procedures used here are not specific to the Nashville urban plume and can be applied to the analysis of O_3 formation in other venues.

Our analysis of the instantaneous chemistry should not be confused with modeling analysis that has been performed on the Nashville data using full scale Eulerian models driven by measured wind fields and emission inventories [e.g., *Sillman et al.*, 1998]. Such modeling exercises have been employed to predict maximum O_3 concentrations and to address the consequences of the reduction of NO_x and/or hydrocarbon emissions on maximum O_3 concentrations. This analysis should not also be confused with the complementary analysis by *Nunnermacker et al.* [1998], which also examines the July 3 and 18 data but uses no model calculations. The analysis presented here examines the processes occurring in the plume at various locations in its evolution to gain a mechanistic understanding of how ozone is being produced. This is accomplished by calculating the concentrations of transient species that were not measured. The calculations make no assumptions about wind fields, emission inventories, and similar parameters but instead use measured concentrations to constrain the calculations. The goal is to examine the instantaneous chemistry occurring in the Nashville plume and how it changes as a function of time, location, and chemical composition as the urban plume advects downwind and ages.

2. Experiment

2.1. Aircraft Flights

A detailed description of the measurements and the meteorological conditions on July 3 and 18 is given by *Nunnermacker et al.* [1998]. Here we briefly restate portions of the conditions relevant to the analysis given below. On July 3, 1995, a weak high-pressure system that had been centered over northern Illinois on July 2 moved to the east, causing the wind to shift from light easterly during the early to midmorning hours of July 3, 1995, to the southwest by the afternoon. Wind speeds determined from the radar profiler just to the NE of Nashville indicated that from 1200 to 1500 LT, winds in the boundary layer were from the (SW) 225° at speeds of 4-5 m/s. These winds carried the Nashville urban plume to the NE of the city. The DOE G-1 aircraft conducted a sampling mission in the Nashville urban area during the early afternoon, 1200-1600 CST. Detailed chemical measurements were made both upwind and downwind of Nashville as indicated by the flight track shown in Plate 1. The Nashville urban plume was encountered approximately 45 and 70 km NE of the Nashville urban center. These distances correspond to processing times of 4.5 and 7.0 hours, respectively. Maximum O_3 concentrations in the plume were of the order of 120 ppbv. O_3 production was nearly complete at the sampling locations as indicated by the low NO_x concentrations (<2 ppbv) which were measured in the center of the plume.

On July 18 a weak cold front passed through the Nashville area during the early hours, bringing relatively clean air to the region. Early in the morning, winds shifted to the N and then to the NE; wind speeds were 4-6 m/s. These winds transported the Nashville
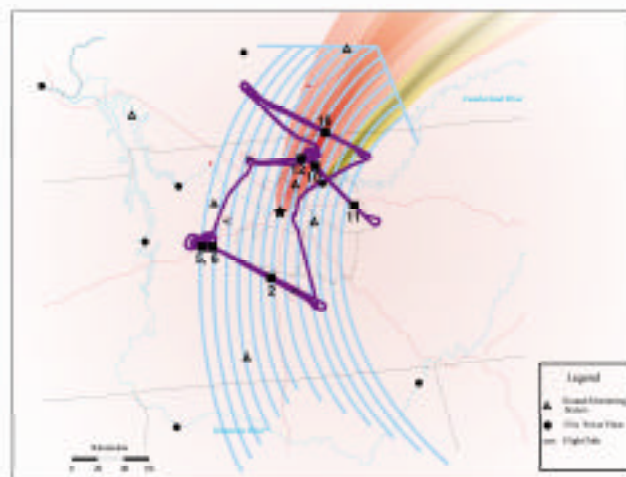

Plate 1.   Ground track of the G-1 flight on July 3, 1995, superimposed on a map of the Nashville area. The light blue arrow shows the average wind direction. The approximate dimensions of the Nashville urban plume and the plume from the Gallatin Power Plant to the NE of Nashville are schematically illustrated in red and yellow, respectively. Locations where hydrocarbon canister samples were collected are indicated by squares. Numbered samples are used in calculations to examine the sensitivity of the ozone production rate to changes in NO_x or hydrocarbon concentrations.
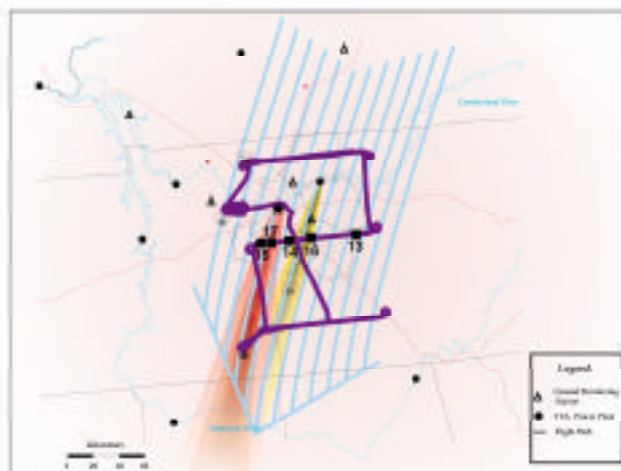

Plate 2. Same as Plate 1 except for the G-1 flight of July 18, 1995.

urban plume to the S and SW of the city. The G-1 sampled the urban area between 1000 and 1400 CDT. The flight track is shown in Plate 2. The urban plume was sampled at approximately 25 km, and 60 km downwind of the city. Plume ages at the sampling locations were approximately 2 and 4 hours. Since the first set of

plume transects was made only 2 hours downwind of the city, only about half the emissions had been processed leading to a maximum O_3 concentration of about 80 ppbv. Further details regarding the chemical composition of the plumes sampled on July 3 and 18, including estimates of the phenomenological rate and efficiency of O_3 production, and conclusions regarding the relative importance of biogenic and anthropogenic hydrocarbons for O_3 production may be found in the work of *Nunnermacker et al.* [1998].

2.2. Model Calculations

Calculations were performed with an observation driven photochemical box model and used steady state approximations as described by *Kleinman et al.* [1997]. The model consists of the kinetic rate expressions for species not constrained to their observed values, i.e., OH, HO_2, organic peroxy radicals, and NO_2. An integration of these equations produces the steady state concentrations of radicals consistent with observed concentrations of stable species. The gas phase photochemical mechanism was based upon the regional acid deposition model (RADM) II [*Stockwell et al.*, 1990] for the oxidation of anthropogenic hydrocarbons and upon the condensed mechanism of *Paulson and Seinfeld* [1992] for the oxidation of isoprene. Input to the model included the observed (from the flights of the G-1) and/or estimated concentrations of hydrocarbons and HCHO (as described below), the observed concentrations of NO, O_3, CO, SO_2, H_2O_2, and organic peroxide, as well as temperature, dew point, and solar intensity.

Calculations correspond to the locations where hydrocarbon canister samples were collected. The locations of these samples are indicated in Plates 1 and 2. Note that samples were collected at various times and locations in the urban plume as well as in the "background" air outside of the plume. Since measurements of HCHO on July 18 were not available, HCHO concentrations were estimated from the relationship between the glyoxal (which was available) and the HCHO concentrations measured on other days [*Lee et al.*, 1998]. Methyl vinyl ketone and methacrolein are set at 250 and 110% of isoprene as appropriate for an equilibrium mixture determined by OH reaction kinetics.

3. Results and Discussion

3.1. Instantaneous Ozone Formation Fates

Figure 1 shows the calculated instantaneous ozone production rate $P(O_3)$ as a function of the NO_x concentration for all of the boundary layer hydrocarbon samples collected on both flights. The circles indicate points corresponding to the July 3 measurements. Open circles correspond to samples collected in background air, solid circles to measurements made in the urban plume. Points corresponding to measurements made on July 18 are shown as diamonds, with solid diamonds indicating the urban plume measurements.

The O_3 production rates in Figure 1 increases almost linearly with the NO_x concentration of up to concentrations of ~2 ppbv. Following a broad maximum, they then decrease when NO_x concentrations exceed ~4 ppbv (see *McKeen et al.* [1991], for a similar picture). Since measurements made on July 3 in the urban plume were taken far downwind from the city center (Plate 1) when emissions had been extensively processed, these data are

grouped in the low NO_x region of Figure 1 and exhibit $P(O_3)$ values indistinguishable from those calculated for background conditions. The high NO_x (>2 ppbv) region of the figure
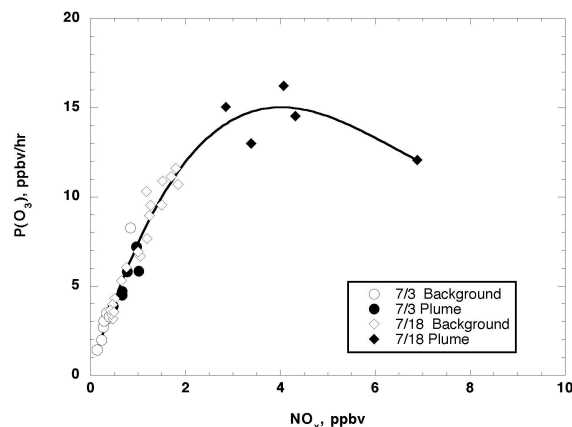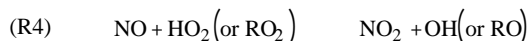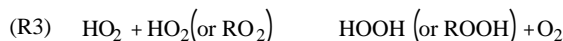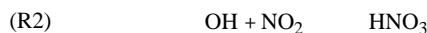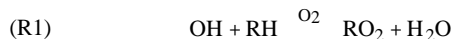

Figure 1. A plot of box-model-calculated O_3 production rates as a function of the observed NO_x concentrations. The calculation is based on data observed on July 3 (circles) and July 18 (diamonds). Background samples are desgnated by the open symbols. At low NO_x, $P(O_3)$ increases almost linearly with NO_x, while above 4 ppbv, increasing NO_x has an inhibiting effect on the O_3 production rate. In this and subsequent figues the solid lines are visual fits to the data.

corresponds to urban plume measurements made on July 18 when only about half the Nashville precursor emissions had been consumed in the production of O_3. Note that $P(O_3)$ and the dependency of $P(O_3)$ on NO_x in the region where data from the two days overlap are nearly identical, suggesting that conditions for O_3 formation were quite similar, and that data from the two days can be interpreted together.

In the discussion below we seek to understand the dependency of $P(O_3)$ on NO_x exhibited in Figure 1. We start with the following four reactions, which represent some of the fundamental processes controlling the rate of atmospheric O_3 production,

(R1) $$OH + RH \xrightarrow{O_2} RO_2 + H_2O$$

(R2) $$OH + NO_2 \longrightarrow HNO_3$$

(R3) $$HO_2 + HO_2 (or\ RO_2) \longrightarrow HOOH\ (or\ ROOH) + O_2$$

(R4) $$NO + HO_2 (or\ RO_2) \longrightarrow NO_2 + OH (or\ RO)$$

and Equations (1) and (2), which are alternate ways of expressing $P(O_3)$ on the basis of the above reactions.

$$P\left(O_3\right) = \frac{k_t}{\left(2\,k_{\text{eff}}\right)^{1/2}}\left(Q - \text{NFR}\right)^{1/2}\left[NO\right] . \qquad (1)$$

$$P\left(O_3\right) = Y\,\frac{k_1\left[HC\right]}{k_2\left[NO_2\right]}\left(Q - 2\text{PFR}\right) . \qquad (2)$$

In equations (1) and (2), k_t is the weighted average rate constant for reaction of HO_2 and RO_2 with NO; k_{eff} is the effective rate constant for peroxide formation; Q is the primary radical production rate (i.e., from the photolysis of O_3 and HCHO); Y is the average yield of $[HO_2] + [RO_2]$ for each OH + RH reaction (G. Tonnesen and R. Dennis, private communication, 1998); k_1 [HC] represents the OH reactivity for the mix of hydrocarbons, including CO, and $k_2[NO_2]$ is the OH reactivity of NO_2, NFR is the nitric acid formation rate,

$$\text{NFR} = k_2\left[NO_2\right]\left[O\,H\right] , \qquad (3)$$

and PFR is the peroxide formation rate,

$$\text{PFR} = k_{\text{eff}}\left[HO_2 + RO_2\right]^2 . \qquad (4)$$

In terms of PFR and NFR the conservation equation for free radicals is given approximately by

$$Q = \text{NFR} + 2\text{PFR} . \qquad (5)$$

Derivation of equation (1), [*Sillman et al.*, 1990; *Kleinman et al.*, 1997] uses equations (4) and (5) and the very good assumption that the ozone production rate is the rate at which NO is oxidized to NO_2 by peroxy radicals, i.e., that

$$P\,(O_3) = k_t\,([HO_2] + [RO_2])\,[NO] \qquad (6)$$

Derivation of equation (2) starts from the assumption that the rate of O_3 production can be approximated by the rate at which OH reacts with hydrocarbons [*Sillman*, 1990; 1995]; that is

$$P\,(O_3) = Y\,k_1\,[OH]\,[RH] . \qquad (7)$$

Equation (7) is valid as long as the chain length for O_3 production is significantly greater than 1, i.e., as long as the peroxy radical produced from OH + RH tends to react with NO rather than with another peroxy radical to form a peroxide. Under the conditions encountered in Nashville, equation (7) is valid for NO_x concentrations above about 1 ppbv. Equation (2) is derived by solving equations (3) and (5) for [OH] in terms of Q, PFR, and NO_2 and substituting this result into equation (7). Both derivations assume steady state conditions, that PAN concentrations are near equilibrium and that losses of radicals by processes other than formation of peroxides or HNO_3 are negligible. Equation (1) is valid for all NO_x concentrations but is most useful for examining the behavior of $P(O_3)$ at low NO_x. Equation (2) is valid except at very low NO_x but is most useful for examining $P(O_3)$ at high NO_x.

In discussing the dependency of $P(O_3)$ on NO_x in Figure 1 it is also useful to have at hand the OH and peroxy radical concentrations calculated by the model, as a function of NO_x, and the rate of nitrate and peroxide formation. These are shown in

Figures 2 through 4. The functional form of the NO_x dependencies of the OH and peroxy radical concentrations, displayed in these figures, resemble those given by *Logan et al.* [1981] and are reasonably well understood.

Our explanation of the NO_x dependency of $P(O_3)$ starts at the left-hand side of Figure 1 where $P(O_3)$ is low and increases linearly with the NO_x concentration. This "low NO_x" region corresponds to samples collected in the mature urban plume sampled on July 3 and to the background samples from both days. In this region of Figure 1, OH radical concentrations are low (Figure 2) and peroxy radical concentrations are high (Figure 3). The nitric acid formation rate is low (Figure 4a) because both the NO_x and the OH concentrations are low. The dominant radical sink is therefore peroxide formation (Figure 4b). Under these conditions, equation (1) reduces to:

$$P\left(O_3\right) = \frac{k_t}{\left(2\,k_{\text{eff}}\right)^{1/2}}\left(Q\right)^{1/2}\left[NO\right] . \qquad (8)$$
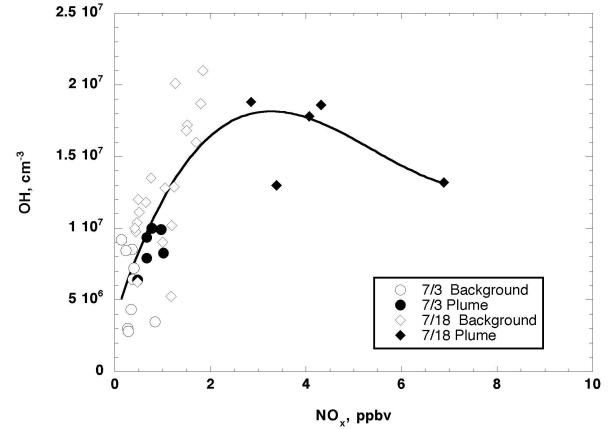

Figure 2. Calculated hydroxy radical concentrations as a function of NO_x. OH concentrations increase by over a factor of 4 when NO_x goes from <0.2 to 4 ppbv, because the rate of NO reaction with peroxy radical to regenerate OH increases. At higher NO_x however, the reaction of NO_2 with OH dominates causing the OH concentrations to decrease. Symbols as for Figure 1.

A plot of $P(O_3)$ as a function of $(Q^{1/2})[NO]$ for all of the data is shown in Figure 5a. $P(O_3)$ for all of the samples collected in the mature urban plume and in the background atmosphere on July 3 and the samples collected in the background on July 18 exhibit the predicted linear low NO_x dependency on $(Q^{1/2})[NO]$. Samples from the relatively fresh urban sampled on July 18 follow a different dependency. This change in dependency may be attributed to a transition between NO_x and hydrocarbon-sensitive O_3 production.

The dependency expressed by equation (8) holds at low NO_x, because at low NO_x, $P(O_3)$ is determined by the competition between (R3) and (R4) for peroxy radicals. The former leads to formation of peroxides, while the latter leads to O_3. It is worth noting that $P(O_3)$ at low NO_x concentrations is insensitive to the
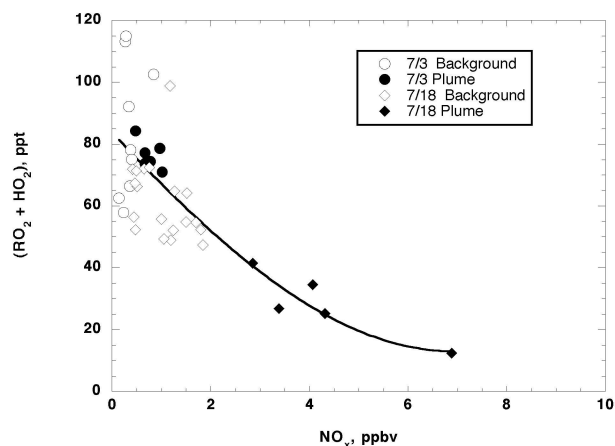
Figure 3.   Calculated total peroxy radical concentrations as a function of NO_x. The peroxy radical concentrations decrease by over an order of magnitude as the NO_x concentrations increase from <0.2 to 8 ppbv. Symbols as for Figure 1.
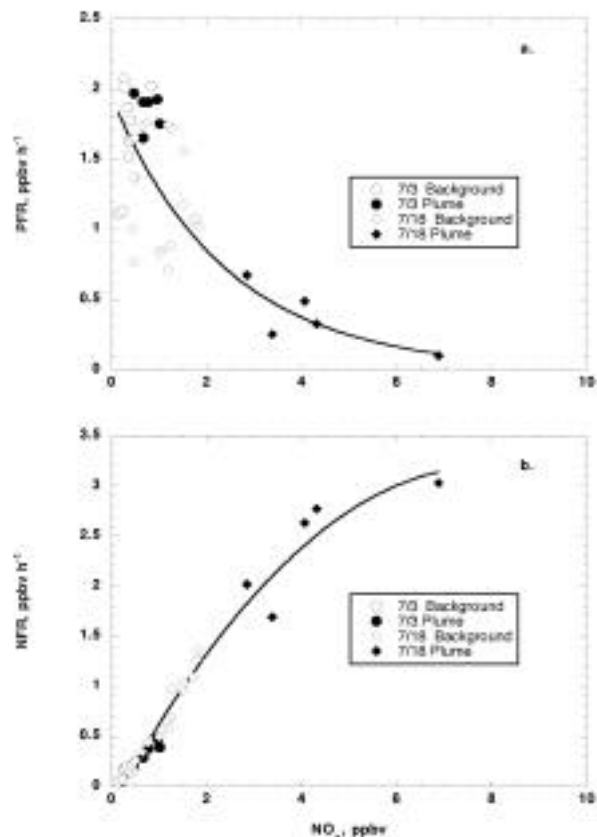

Figure 4.   Comparison of the importance of the two radical sink pathways as a function of the NO_x concentration. At low NO_x the dominant termination pathway is through peroxide formation, while at high NO_x, the chain reactions terminate mostly by nitrate formation. Symbols as for Figure 1.

hydrocarbon reactivity. In the linear, low NO_x portion ($NO_x < 0.5$ ppbv), of Figure 5a, the hydrocarbon reactivity varies by over a factor of 10, as shown in Figure 6, but $P(O_3)$ is not sensitive to these variations because (R1) is not the rate-limiting step for O_3 production.
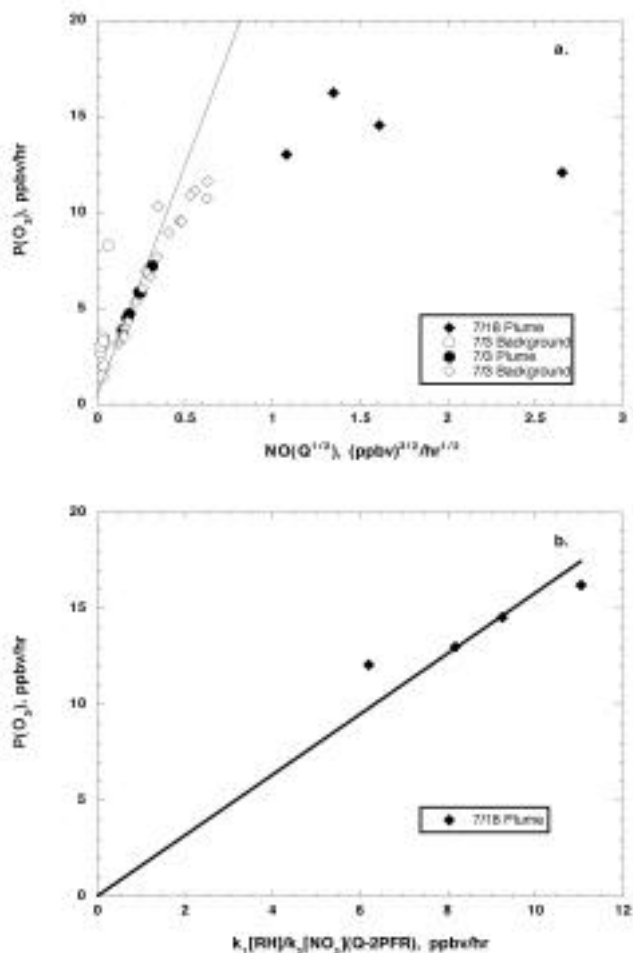

Figure 5. (a) Ozone production rate as a function of the product of the NO concentration and the radical production rate. $P(O_3)$ follows the linear behavior predicted by equation (8) up to a NO_x concentration of 2 ppbv. Equation (8) breaks down at higher NO_x concentrations; (b) Ozone production rate as a function of the product of Q and the ratio of the hydrocarbon to NO_x, OH reactivity. This linear dependency holds for the high NO_x samples collected in the 2 hour old plume sampled on July 18.

At NO_x values to the right of the $P(O_3)$ maximum, all of which may be identified with the 2 hour old urban plume sampled on July 18, the decrease in $P(O_3)$ at high NO_x concentrations can be attributed to direct competition between hydrocarbons and NO_2 for OH, (R1) versus (R2). When OH reacts with a hydrocarbon, one or more peroxy radicals are formed, and O_3 is produced by (R4).
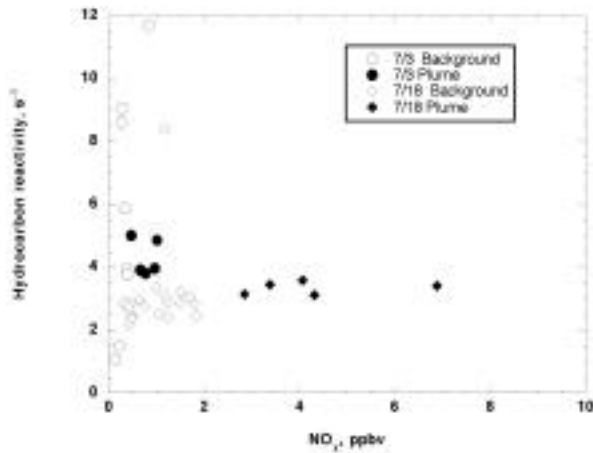
Figure 6. Distribution of the hydrocarbon reactivity for the two days plotted as a function of NO_x. Symbols as for Figure 1. No systematic dependence of this reactivity on NO_x is observed.

When the OH reacts with NO_2 to form HNO_3, it is lost from the system. In the high NO_x region, nitric acid formation is the dominant termination pathway (see Figure 4), PRF   0 and 2 reduces to

$$P\left(O_3\right) = Y\frac{k_1\left[RH\right]}{k_2\left[NO_2\right]}Q \ , \qquad (9)$$

showing that at high NO_x, $P(O_3)$ is directly proportional to the ratio of the hydrocarbon to NO_x, OH reactivity [see *Sillman et al.*, 1990, equation (5)]. In Figure 5b we have plotted $P(O_3)$ as a function of the quantity $k_1[RH]/k_2[NO_2](Q$-2PFR), equation (2), instead of $k_1[RH]/k_2[NO_2]Q$ as peroxide formation for these samples consumed as much as 25% of Q. This plot exhibits the expected linear dependency of $P(O_3)$ on the ratio of the hydrocarbon to NO_2, OH reactivity. The slope of 1.6 may be interpreted as the average number of peroxy radicals that result from the reaction of OH with the ambient mix of hydrocarbons.

At low NO_x, equation (8) shows that $P(O_3)$ is directly proportional to [NO], while at high NO_x, equation (9) shows that $P(O_3)$ is inversely proportional to $[NO_2]$. Continuity dictates that $P(O_3)$ have a maximum at some intermediate values of NO_x. This maximum occurs at a NO_x concentration such that NFR/Q = 2/3, or more explicitly when two thirds of the radicals are being sunk as nitric acid and one third as peroxide [*Kleinman et. al.*, 1997]. The NO_x concentration where this occurs is about 4 ppbv on July 18, but will vary according to the chemical environment.

3.2. O_3 Production Efficiencies With Respect to NO_x (OPE$_x$)

Nunnermacker et al. [1998] calculated the mean O_3 production efficiency with respect to NO_x (OPE$_x$) in the Nashville urban plume from the ratio of the amount of O_3 produced to the amount of NO_x that had been consumed at the location where the plume had been sampled. The mean OPE$_x$ in the mature urban plume

sampled on July 3 was found to be 4 ppbv O_3/ppbv of consumed NO_x, and for the plume sampled on July 18, 2 ppbv O_3/ppbv NO_x.

Here we examine the instantaneous values of this quantity and its dependence on the NO_x concentrations. The instantaneous OPE$_x$ is defined as follows:

$$OPE_x = \frac{P\left(O_3\right)}{d\left(NO_z\right)/dt} = \frac{P\left(O_3\right)}{P\left(NO_z\right)} \qquad (10)$$

where in equation (10), $NO_z = NO_y - NO_x$, and the other terms have their previous definition. Figure 7 shows the instantaneous OPE$_x$ calculated by the box model for each of the hydrocarbon canister samples, plotted as a function of the measured NO_x concentration. The OPE$_x$ is high at low NO_x and decreases monotonically with increasing NO_x concentration. Thus O_3 is produced more efficiently per NO_x, in the background and in the NO_x-depleted mature urban plume on July 3, than it is in the relatively fresh urban plume sampled on July 18. However, while O_3 is produced more efficiently at low NO_x, the availability of NO_x limits the amount of O_3 that can be formed. It is also important to understand that the values of $P(O_3)$, which are discussed here, do not include O_3 loss rates (for example, from photolysis). Under low NO_x, high O_3 conditions, as pertain, for example, to the mature urban plume sampled on July 3, the net O_3 production efficiency can be much lower than OPE$_x$.
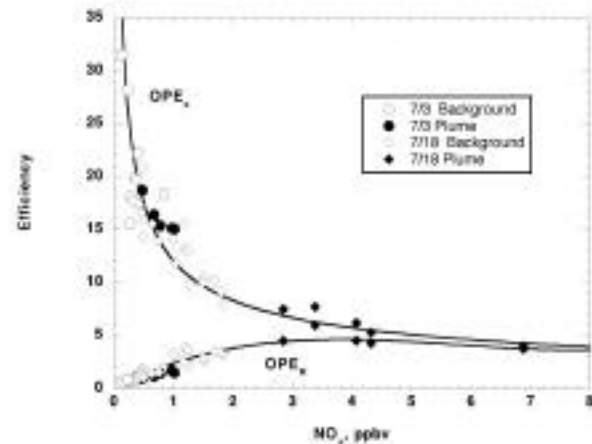

Figure 7. O_3 production efficiencies calculated from the box model, with respect to NO_x, OPE$_x$, and with respect to primary radicals, OPE$_R$ as a function of NO_x. At low NO_x, OPE$_R$ increases, and OPE$_x$ decreases with NO_x. At high NO_x where radical removal is dominated by nitrate formation the two efficiencies converge (see explanation in text).

This NO_x dependency of OPE$_x$ is a manifestation of the dual role that NO_x plays in the photolytic cycle in which it is essential for O_3 production while at the same time acts to "poison" the photolytic cycle by competing with a hydrocarbon for OH through the termination reaction (R2). The OPE$_x$ can also be viewed approximately as a measure of the number of times an OH radical reacts with a hydrocarbon molecule as compared to an NO_2

molecule adjusted for the number of peroxy radicals produced by the reaction of OH with a hydrocarbon:

$$OPE_x = Y \frac{k_1[RH]}{k_2[NO_2]} .$$ (11)

Figure 8 shows a plot of OPE_x as a function of the hydrocarbon to NO_x reactivity ratio. The data follow equation (11) up to hydrocarbon to NO_x reactivity ratios of about 15.
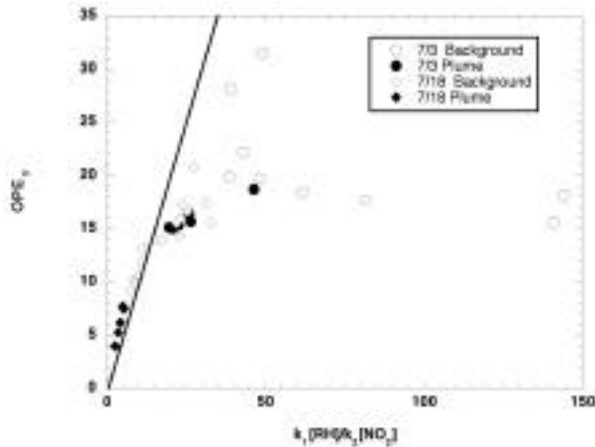

Figure 8. OPE_x as a function of the hydrocarbon to NO_x reactivity ratio. OPE_x increases linearly up to a reactivity ratio of approximately 15; above 15, OPE_x becomes independent of this ratio.

3.3. O$_3$ Production Efficiency With Respect to Radicals (OPE$_R$)

The importance of OPE_x to control strategies is straightforward. There is however, a second type of ozone production efficiency that can provide a great deal of insight into the photochemical processes forming tropospheric O_3. In the photochemical cycle that produces O_3, two species are catalysts and therefore are regenerated at the end of each cycle. The first is NO, and OPE_x is a measure of the number of times an NO molecule goes around the photolytic cycle. The second catalyst is OH, or in more general terms, odd hydrogen radicals. Similar to OPE_x, the O_3 production efficiency with respect to radicals (OPE_R) is a measure of how many times a primary radical participates in the O_3 formation process. The instantaneous OPE_R can be defined as the ratio of the O_3 and radical production rates

$$OPE_R = \frac{P(O_3)}{Q} = Y \frac{k_1[RH]}{k_2[NO_2]} \left(1 - 2\frac{PFR}{Q}\right) ,$$ (12)

in which the term $2(PFR/Q)$ represents the fraction radicals that are removed in the form of peroxides.

At high NO_x concentrations the fraction of radicals that are removed by peroxide formation is very small and equation (12) reduces to:

$$OPE_R = \frac{P(O_3)}{Q} = Y \frac{k_1[RH]}{k_2[NO_2]} \text{ and } OPE_R \approx OPE_x .$$ (13)

At very low NO_x concentrations where almost all of the radicals form peroxides, Figure 4, $P(O_3)$ is given by equation (8) and the dependency of OPE_R on NO_x takes the form:

$$OPE_R = \frac{P(O_3)}{Q} = \frac{k_t}{(2 k_{eff})^{1/2}} \frac{[NO]}{Q^{1/2}} .$$ (14)

For comparative purposes the dependency of OPE_R on NO_x is superimposed on the plot of OPE_x in Figure 7. As indicated by equation (13), OPE_R and OPE_x are nearly identical at high NO_x concentrations. As the NO_x concentrations decrease, OPE_R goes through a maximum, then decreases toward zero as the NO_x concentrations become very small. This variation of OPE_R on NO_x is very similar to the NO_x dependency of $P(O_3)$, exhibited in Figure 1. The explicit dependency of OPE_R on NO at low NO concentrations is shown in Figure 9 where the linear behavior predicted by equation (14) at low NO_x is observed. Thus in the context of the Nashville urban plume, radicals are most efficiently used in formation of O_3 near the $P(O_3)$ maximum.
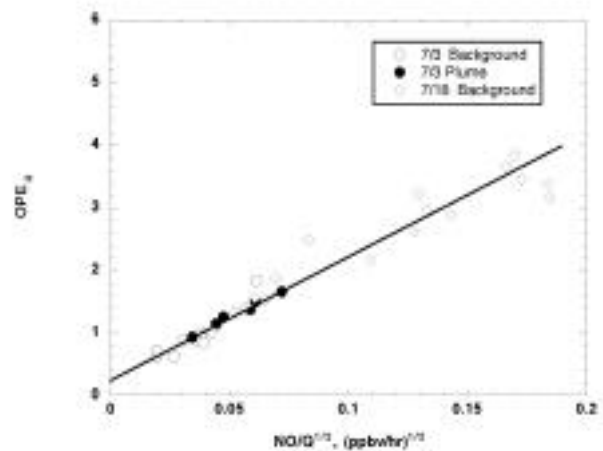

Figure 9. Ozone production efficiency with respect to radicals as a function of $NO/Q^{1/2}$ for samples collected in the background and in the mature urban plume on July 3 and in the background on July 18. Since Q was relatively constant for these samples, plot indicates that OPE_R is a linear function of NO_x at low NO_x.

3.4 NO$_x$ and Hydrocarbon Limitations to $P(O_3)$

Insight into the issue of NO_x or hydrocarbon limitations in the background air surrounding Nashville and in the Nashville plume at various stages of its development is explored in this section. This study was conducted as follows: First, $P(O_3)$ was calculated using our box model for each of the hydrocarbon samples using observed trace gas concentrations. In the second set of calculations, either the NO_x or the hydrocarbon concentrations were decreased by 10% while keeping the rest of the concentrations fixed (the 10% reduction in hydrocarbons included

anthropogenic as well as biogenic hydrocarbons, except for formaldehyde which was kept at its observed value). The difference between the O_3 production rates under the three sets of conditions allows examination of the sensitivity of the system to changes in O_3 precursor concentrations.

We first examine the results corresponding to the flight of July 3. Since the urban plume measurements on this flight were made when the plume was 4-7 hours downwind of the source region, O_3 concentrations were near their maximum, and virtually all the NO_x had been consumed. In addition to the urban plume, calculations were also performed for samples collected outside of the plume in "background" air. The background samples were divided into two groups according to their isoprene concentrations (the two isoprene regimes have been described by *Nunnermacker et al.* [1998]). The locations of the hydrocarbon samples for which these calculations were done are indicated in Plate 1.

The results of the sensitivity calculations for July 3 are shown in Figure 10. The open bars in Figure 10 depict the calculated instantaneous O_3 production rate (not including O_3 losses of the order of 2 ppbv/h) for the base case. The background production
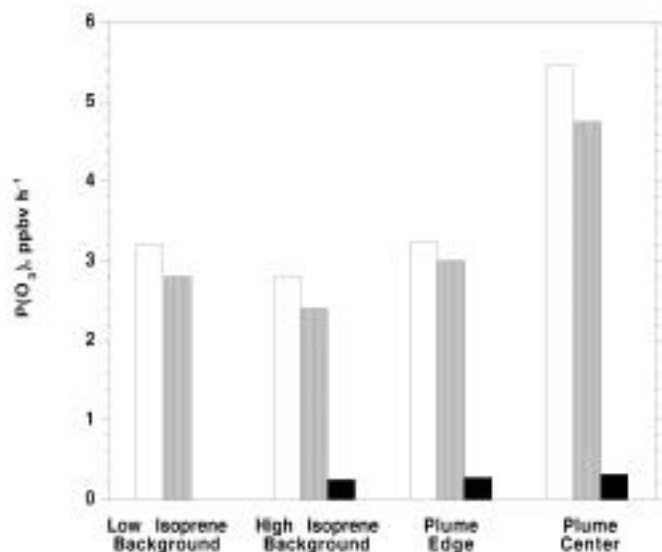

Figure 10. Sensitivity of the instantaneous O_3 production rate (not including O_3 losses) to changes in either NO_x or ROG emissions on July 3 calculated from box model which used trace gas observations coincident with ROG samples specified at the bottom of the graph. The open bars represent the base case scenario. O_3 production rate in the background were ~3 ppbv/h and at the plume center slightly higher. The shaded/solid bars represent the systems response to a 10% decrease in NO_x or ROG, respectively. The relative height of a shaded/solid bar with respect to its counterpart open bar (base case) is a measure of the sensitivity of the O_3 production rate to changes in NO_x or ROG concentrations. If a shaded/solid bar has a height equal to the base case, this implies that a 10% decrease in emissions leads to a 10% decrease in the ozone production rate, i.e., a maximum response. All of the data from July 3 are in the NO_x-sensitive regime. Location of hydrocarbon samples is shown in Plate 1.

rate is ~3 ppbv/h for both the low- and the high-isoprene background data. Despite the fact that there is a factor of 3 difference in hydrocarbon reactivity, between the high- and the low-isoprene background samples it has little effect on $P(O_3)$, because $P(O_3)$ in the background is entirely controlled by the NO_x concentration. At the center of the plume the ozone production rate is slightly higher (5.5 ppbv/h) than for the background samples because the NO_x concentration is higher.

The sensitivity of the system to a 10% decrease in either NO_x or hydrocarbon concentrations is depicted by the shaded bars for NO_x and solid bars for hydrocarbons. The ratio of the height of either a shaded or a solid bar with respect to its counterpart open bar (base case) is a measure of the sensitivity of the O_3 production rate to changes in NO_x or hydrocarbon concentrations. If the bar corresponding to the perturbed concentrations has a height equal to the base case, this implies that a 10% decrease in emissions leads to a 10% decease in the ozone production rate, i.e., a maximum response. Conversely, a test bar that is only 10% of its counterpart base case bar implies that a 10% reduction in concentration would lead to only a 1% change in the O_3 production rate, i.e., that the system is insensitive to the change in concentrations. In some cases the sensitivity can be negative. In these cases a decrease in concentration has the effect of increasing the O_3 production rate. Similarly, the ratio of the two test bars is a measure of the relative efficiency with which the O_3 production rate can be influenced via a change in NO_x or hydrocarbons. It is important to stress that these sensitivity tests relate only to the instantaneous chemistry and do not reflect the sensitivity of the overall or maximum O_3 concentrations to changes in the NO_x or hydrocarbon emissions.

For the data of July 3rd presented in Figure 10, we find that the shaded bars (sensitivity to NO_x) were consistently within 90% of the open bars. This indicates that for all locations, whether in or out of the urban plume, $P(O_3)$ is close to maximally sensitive to reduction in the NO_x concentrations. Conversely, the small solid bars (sensitivity to hydrocarbons) indicate that the system is insensitive to changes in hydrocarbon concentrations. This conclusion is consistent with chemical age of the urban plume as indicated by the fact that more than 80% of the NO_x has already been consumed.

The equivalent sensitivity data for the flight segment just south of the urban center on July 18 (Plate 2) are shown in Figure 11. Because the urban plume was sampled only 2 hours downwind of the urban center, when only about half of the NO_x and slightly more than half of the anthropogenic hydrocarbons had been consumed, these calculations give a view of the processes that control O_3 at an intermediate stage in its production. The data in Figure 11 include four samples collected at various points in the plume as well as a background sample. The open bars show that at the center of the urban plume, O_3 production rates are nearly 3 times higher than those on July 3. This is due to the much higher NO_x concentration. The background O_3 production rates on the two days were similar.

In Figure 11, the background sample 13 exhibits NO_x sensitive chemistry. At the plume edges represented by the two outermost samples 15 and 16, where NO_x concentrations are relatively low, the O_3 production rate is more sensitive to changes in NO_x than to changes in the hydrocarbons. However, as indicated by the height of the gray bars relative to the open bars, a 10% decrease in NO_x concentration produces significantly less than an equivalent decrease in the O_3 production rate. In sample 14, for example, O_3

production rate decreases by only 4.5% in response to the 10% decrease in NO$_x$ concentrations. The O$_3$ production rates for the
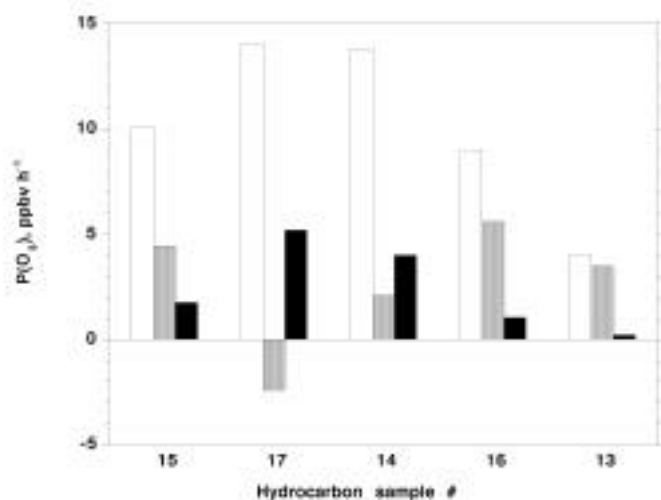

Figure 11. Sensitivity of the instantaneous O$_3$ production rate (not including O$_3$ losses) to changes in either NO$_x$ or ROG emissions on July 18. For an explanation of the figure legend see Figure 5. Samples 14 through 17 were taken with a relatively fresh urban plume in which about half of the NO$_x$ was still present. Samples 15 and 16 taken near the plume edge show slightly higher sensitivity to NO$_x$ than to hydrocarbons but the sensitivity is low. Sample 14 near the plume center exhibits a higher ROG than NO$_x$ sensitivity, however both sensitivities are very low. Note that at the plume center, decreasing NO$_x$ concentrations have the effect to increase the O$_3$ production rate. Location of hydrocarbon samples is shown in Plate 2.

two samples at the center of the urban plume (samples 17 and 14) exhibit a greater sensitivity to hydrocarbons than for NO$_x$. Moreover, for sample 17, collected at center of the plume where NO$_x$ concentrations are highest, the O$_3$ production rate increases in response to a slight decrease in NO$_x$ concentration. At this point the O$_3$ production rate is clearly more sensitive to decreases in hydrocarbons than to NO$_x$, but this sensitivity is low, as indicated by the relative height of the solid and open bars. This implies that a meaningful impact on the O$_3$ production rate at this stage would require significant decreases in either the hydrocarbon or the NO$_x$ emissions.

These two samples of urban plume chemistry taken when about half and nearly all the Nashville emissions had been consumed, when combined with a similar calculations for the downtown data, illustrate the evolution of the sensitivity of O$_3$ production to hydrocarbon and NO$_x$. The system starts at the urban center being entirely hydrocarbon sensitive, when about half of the NO$_x$ emissions have been consumed, the center of the evolving plume is still under hydrocarbon control but with diminished sensitivity to changes in this quantity. As more of the NO$_x$ is consumed, the system eventually becomes NO$_x$ sensitive.

4. Summary and Conclusions

A series of calculations of $P(O_3)$ and related quantities using a box model constrained by measured concentrations of stable species have been made to develop a mechanistic understanding of the chemical processes forming O$_3$ in the Nashville urban plume as it advects downwind, reacts, and produces O$_3$. It was found that at high NO$_x$ concentrations corresponding to the relatively fresh (~2 hour transit time) urban plume sampled on July 18 that $P(O_3)$ was directly proportional to $k_1[HC]/k_2[NO_2]$. At lower NO$_x$ concentrations corresponding to the mature urban plume sampled on July 3 (5-8 hour transit time) and to samples collected in background on both days, $P(O_3)$ was found to be directly proportional to the NO$_x$ concentration and independent of the hydrocarbon reactivity even though the hydrocarbon reactivity varied by a factor of 10.

The dependencies of the instantaneous O$_3$ production efficiencies with respect to both NO$_x$ and to the primary radical production rate Q were examined. The calculations show that OPE$_x$ was very high in the background and in the mature urban plume when NO$_x$ concentrations were low decreased monotonically with increasing NO$_x$ concentration, and was lowest in the center of the fresh urban plume sampled on July 18. The high values of OPE$_x$ at low NO$_x$ were attributed to the low OH concentrations which minimized losses of NO$_x$ by reaction with OH to form HNO$_3$. As the NO$_x$ concentrations increase, NO$_x$ starts to compete with the hydrocarbons for OH by forming HNO$_3$. This terminates the O$_3$ formation cycle and causes the efficiency to decrease. At high NO$_x$ concentrations, OPE$_x$ was found to be proportional to the ratio of the hydrocarbon to NO$_x$ reactivity.

The efficiency with which the primary radicals are utilized, OPE$_R$, is also dependent on NO$_x$, being low at low NO$_x$, going through a maximum at a NO$_x$ concentration of ~4-5 ppbv and thereafter decreasing with increasing NO$_x$. The low efficiency of radical utilization at low NO$_x$ is attributed to peroxide formation, which at low NO$_x$ effectively competes with NO for peroxy radicals. At high NO$_x$ concentrations, OPE$_R$ decreases as the NO$_x$ concentration increases as a result of a competition between ROG and NO$_2$ for OH. In the limit of high NO$_x$, OPE$_x$ = OPE$_R$.

The relative sensitivity of the O$_3$ production rate to NO$_x$ and ROG was examined from several perspectives. On July 18 when measurements were made early in the processing of the Nashville urban emissions (only half of the NO$_x$ had been consumed), $P(O_3)$ was found to be hydrocarbon sensitive at the center of the urban plume. At this stage in the chemical evolution of the plume, a small reduction in NO$_x$ concentration has the effect of increasing $P(O_3)$. However, in the mature urban plume sampled on July 3 where NO$_x$ concentrations were low, $P(O_3)$ became limited by the availability of NO$_x$. In background air on both days, NO$_x$ concentrations were low and $P(O_3)$ was always limited by the availability of NO$_x$.

References

Kleinman, L., Y.-N. Lee, S. R. Springston, J. H. Lee, L. Nunnermacker, J. Weinstein-Lloyd, X. Zhou, and L. Newman, Peroxy radical concentration and ozone formation rate at a rural site in the southeastern United States, *J. Geophys. Res., 100*, 7263-7273, 1995.

Kleinman, L. I., P. H. Daum, J. H. Lee, Y.-N. Lee, L. J., Nunnermacker, S. R. Springston, L. Newman, J. Weinstein-Lloyd, and S. Sillman, Dependence of ozone production on NO and hydrocarbons in the troposphere, *Geophys. Res. Lett., 24*, 2259-2302, 1997.

Kleinman, L. I., P. H. Daum, J. H. Lee, Y.-N. Lee, J. Weinstein- Lloyd, S. R. Springston, M. Buhr, and B. T. Jobson, Photochemistry of O_3 and related compounds over southern Nova Scotia, *J. Geophys. Res., 103*, 13,519-13,529, 1998.

Lee, Y.-N., et al., Atmospheric chemistry and distribution of formaldehyde and several multioxygenated carbonyl compounds during the 1995 Nashville/Middle Tennessee Ozone Study, *J. Geophys. Res., 103*, 22,449-22,462, 1998.

Logan, J. A., M. J. Prather, S. C. Wofsy, and M. B. McElroy, Tropospheric chemistry: A global perspective, *J. Geophys. Res., 86*, 7210-7254, 1981.

McKeen, S. A., E. Y. Hsie, M. Trainer, R. Tallamraju, and S.C. Liu, A regional model study of the ozone budget in the eastern United States, *J. Geophys. Res., 96*, 10,809-10,845, 1991.

Nunnermacker, L. J., et al., Characterization of the Nashville urban plume on July 3 and July 18, 1995, 1, O_3 production efficiency, kinetic analysis, and hydrocarbon apportionment, *J. Geophys. Res, 103*, 28,129-28,148, 1998.

Paulson, S. E., and J. H. Seinfeld, Development and evaluation of a photochemical mechanism for isoprene, *J. Geophys. Res., 97*, 20,703-20,715, 1992.

Sillman, S., Use of NO_y, HCHO, H_2O_2, and HNO_3 as indicators for ozone-NO_x-hydrocarbon sensitivity in urban locations, *J. Geophys. Res., 100*, 14,175-14,188, 1995.

Sillman, S., J. A. Logan, and S. C. Wofsy, The sensitivity of ozone to nitrogen oxides and hydrocarbons in regional ozone episodes, *J. Geophys. Res., 95*, 1837-1851, 1990.

Sillman, S., D. He, M. Pippin, P. H. Daum, J. H. Lee, L. Kleinman, and J. Weinstein-Lloyd, Model correlations for ozone, reactive nitrogen, and peroxides for Nashville in comparison with measurements: Implications for O_3-NO_x-hydrocarbon chemistry, *J. Geophys. Res., 103*, 22,629-22,644, 1998.

Stockwell, W. R., P. Middleton, J. S. Chang, and X. Tang, The second generation regional acid deposition model chemical mechanism for regional air quality modeling, *J. Geophys. Res., 95,* 16,343-16,347, 1990.

_____

P. H. Daum, D. G. Imre, L. Kleinman, Y.-N. Lee, L. Newman, L. J. Nunnermacker, and S. R. Springston, Environmental Chemistry Division, Department of Applied Science, Brookhaven National Laboratory, Upton, NY 11973-5000. (phdaum@bnl.gov)

J. Weinstein-Lloyd, Dept. of Chemistry and Physics, State University of New York, Old Westbury, NY 11586.